Supplementary Information (SI) for Environmental Science: Nano.
This journal is © The Royal Society of Chemistry 2024

Supporting Information

Transformation of iron oxides in amorphous nanoscale zero-valnent iron (A-nZVI) and nZVI: effect on Sb(III) removal affinity and stability

Qi Cheng,[1ab] Qingrui Li,[1ab] Xiaoqin Li,[*ab] Weizhen Liu[ab], Zhang Lin[cd] and Liyuan Chai[cd]

[a] School of Environment and Energy, Guangdong Provincial Key Laboratory of Solid Wastes Pollution Control and Recycling, South China University of Technology, Guangzhou, Guangdong 510006, PR China

[b] The Key Laboratory of Pollution Control and Ecosystem Restoration in Industry Clusters (Ministry of Education), South China University of Technology, Guangzhou 510006, PR China

[c] Institute of Environmental Engineering, School of Metallurgy and Environment, Central South University, Changsha 410083, China

[d] Chinese National Engineering Research Center for Control & Treatment of Heavy Metal Pollution, Changsha 410083, China

[1] These authors contributed equally to this work

* Corresponding authors: Xiaoqin Li, School of Environment and Energy, South China University of Technology, Guangzhou 510006, PR China

E-mail address: xqli306@scut.edu.cn

Pages: 9, Figures: 5, Table: 2

Text S1

Desorption experiments:

After the adsorption experiments (pH = 5 ± 0.2, Sb(III) initial concentration 100 mg/L, 4 h), the precipitate was separated by centrifugation and washed three times with deionized water for desorption experiments. 100 mL deionized water was added and shaken at 200 r/min (25°C). At the preset time intervals (1, 2, 4, 8, 16, 24, 48 h), 1.0 mL mixture was taken from the bottles and filtered in a 10 mL centrifuge tube with a 0.22 μm syringe filter. The concentration of Sb in the solution was detected by ICP-OES, and the desorption rate (%) was calculated by 100 × (the amount of Sb desorbed/the amount of Sb adsorbed). The experiments were conducted in triplicate.

XAFS testing and analysis：

The XAFs data of Sb-containing solid samples after reaction equilibrium were collected at the 4W1B line station of the Beijing Synchrotron Radiation Facility (BSRF) of the Institute of High Energy Physics, Chinese Academy of Sciences and the synchrotron radiation source (SSRF) X-ray fine structure station (BL14W1) of the Shanghai Institute of Applied Physics, Chinese Academy of Sciences. The K-edge XAFS data of Fe were collected by BSRF, and the pretreatment analysis was performed by Athena software. The contribution of different iron oxides in each sample was analyzed by Linear Combination Fitting (LCF), and the content of various iron oxides was obtained.

Data reduction, data analysis, and EXAFS fitting were performed with the Athena and Artemis software packages.[1] A linear function was subtracted from the pre-edge region, then the edge

jump was normalized using Athena software. The χ(k) data were isolated by subtracting a smooth, three-stage polynomial approximating the absorption background of an isolated atom. The k3-weighted χ(k) data were Fourier transformed after applying a Hanning window function (Δk = 1.0). For EXAFS modeling, the global amplitude EXAFS (*CN, R,* S_0^2, σ^2 and ΔE_0) were obtained by nonlinear fitting, with least-squares refinement, of the EXAFS equation to the Fourier-transformed data in R-space, using Artemis software. The obtained amplitude reduction factor S_0^2 value (0.900) was set in the EXAFS analysis to determine the coordination numbers (CNs) in the Sb-O/Fe scattering path in sample.[2]

Note: The FTs of the EXAFS spectra isolate the contributions of different coordination shells, in which the peak positions correspond to the interatomic distances and the intensity of the peak is related to the contribution of the atoms to the shell. However, the peak positions in Figure 5 have not been corrected for the phase shift effects and thus they deviate from the real distance by 0.3–0.5 Å.

Density functional theory (DFT) analysis：

The DFT calculations are performed with the Vienna ab-initio Simulation Package (VASP). The Perdew-Burke-Ernzerhoff (PBE) functional of the generalized gradient approximation (GGA) scheme was employed to describe the exchange–correlation interaction.[3] The cutoff energy was set as 500 eV to gain the converged results during calculations. For all substrate and adsorption system calculations, a converged (2×2×1) Monkhorst–Pack k-point set is used to sample the total energy. The convergence criteria for structure optimization and energy calculation are set as follows: (a) the energy tolerance is 2.0×10^{-5} eV/atom; (b) the maximum

displacement tolerance is 0.002 Å, and (c) the maximum force tolerance is 0.05 eV/Å.

The adsorption energies (Eads) were calculated by the density functional theory (DFT) calculations as Eads= Ead/sub -Ead -Esub, where Ead/sub, Ead, and Esub are the total energies of the optimized adsorbate/substrate system, the adsorbate in the structure, and the clean substrate, respectively. Because electronic correlations play an important role in transition-metal oxides, an on-site Coulomb repulsion parameter U within the GGA+*U* approach is included. Strong on-site electron correlation was considered for the electrons in Fe of the Fe_3O_4 d-orbitals employing the rotationally invariant DFT+*U* formalism with U_{eff} = 3.61 eV and others Fe employing the rotationally invariant DFT+*U* formalism with U_{eff} = 3.0 Ev.[4]

Table S1 Raman characteristic peaks of iron (hydrogen) oxides

Iron (hydrogen) oxides	Raman shift (cm^{-1})
Magnetite (Fe_3O_4)	316, 540, 686
Hematite (α-Fe_2O_3)	210, 276, 400, 601,
Maghematite (γ-Fe_2O_3)	350, 700
Goethite (α-FeOOH)	299, 385, 479, 581
Lepidocrocite (γ-FeOOH)	245, 385, 522, 658

The above are the typical Raman characteristic peaks of iron oxides.[5,6]

Table S2 Fitting parameters derived from EXAFS Spectra analysis at the Sb K-edge of nZVI and A-nZVI after reacting with Sb(III).

Sample	Shell	CN[a]	R(Å)[b]	σ^2(Å^2)[c]	ΔE_0(eV)[d]	R factor
A-nZVI-Sb	Sb-O	4.4	1.98	0.004	6.6	0.009
	Sb-Fe	1.2	3.16	0.011		
nZVI-Sb	Sb-O	4.6	1.98	0.004	6.2	0.007
	Sb-Fe	0.7	3.17	0.008		

[a]*CN*，coordination number; [b]*R*，the distance between the absorption atom and the backscattered atom; [c]σ^2，Debye-Waller factor to explain thermal and structural disorders; [d]ΔE_0，Internal potential correction; *R* factor，goodness-of-fit. S_0^2 is set to 0.900 according to the empirical value. (S_0^2=0.900)

Fitting range：$3.0 \le k(/Å) \le 13.7$，$1.0 \le R(Å) \le 3.5$ (A-nZVI-Sb(Ⅲ))；$3.0 \le k(/Å) \le 12.8$，$1.0 \le R$ (Å) ≤ 3.5 (nZVI-Sb(Ⅲ)).

A reasonable range of EXAFS fitting parameters: 0.700 < S_0^2 < 1.000; CN > 0; σ^2 > 0 Å^2; ΔE_0 < 10 eV; R factor < 0.02.

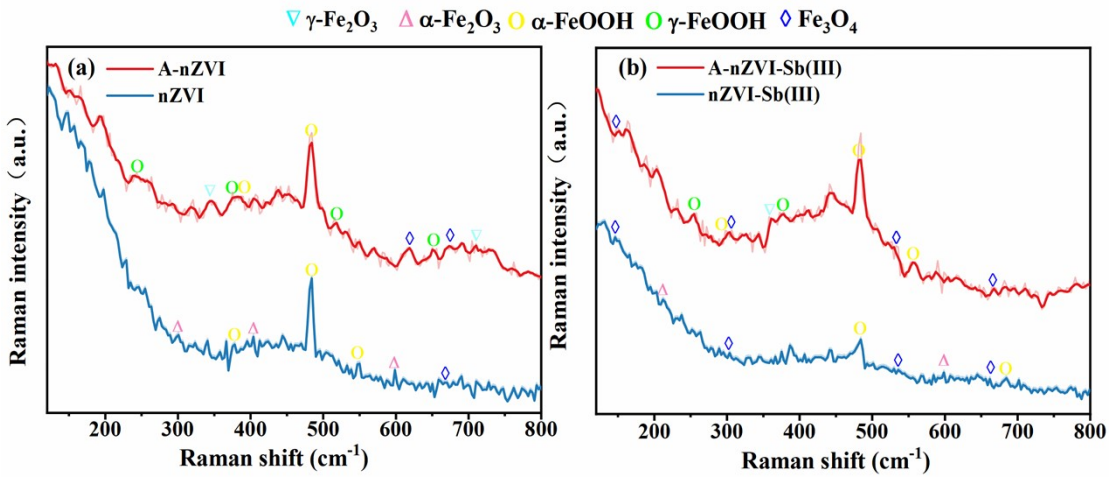

Fig. S1. Raman spectra of nZVI and A-nZVI before and after reaction.

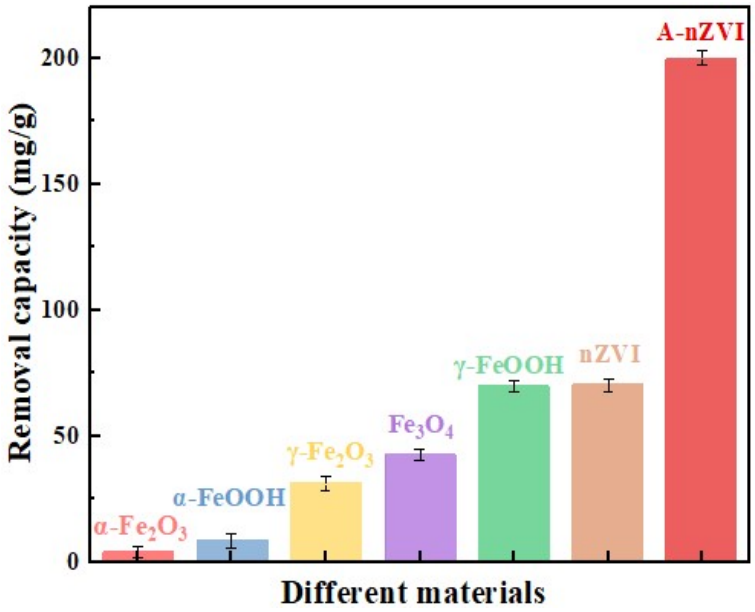

Fig. S2. Comparison of removal capacity of Sb(III) by nZVI, A-nZVI and five iron oxides.

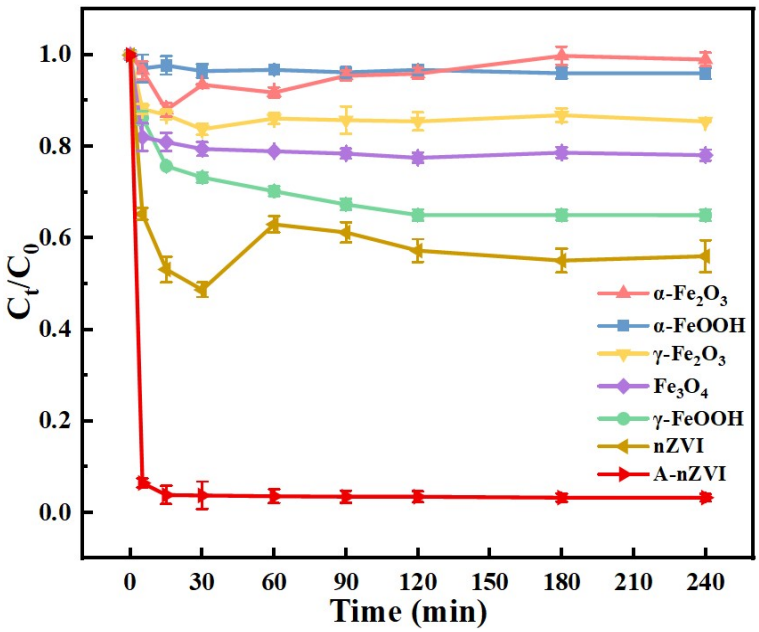

Fig. S3. Removal kinetics of Sb(III) by nZVI, A-nZVI and five iron oxides.

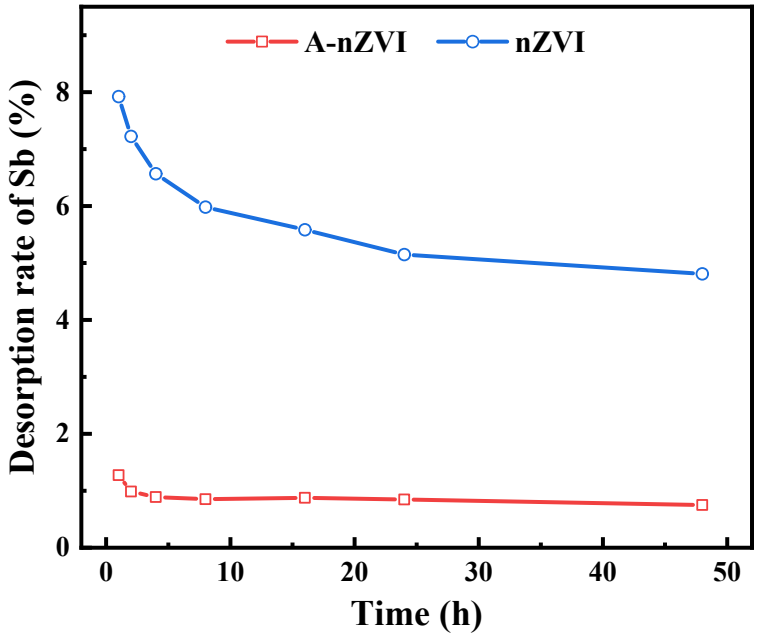

Fig. S4. Desorption rate of Sb for A-nZVI and nZVI (desorption solution: deionized water, V: 100 mL, [A-nZVI]/[nZVI]: 0.5 g/L, T: 25±1℃)

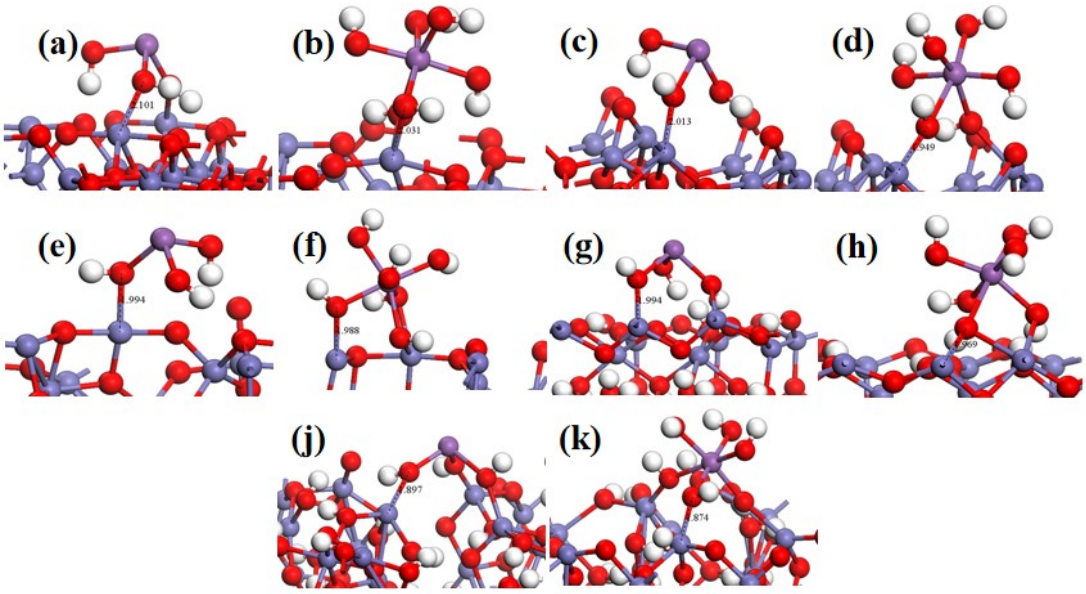

Fig. S5. DFT calculation model for the adsorption of Sb(III) ($Sb(OH)_3$) and Sb(V) ($Sb(OH)_6^-$) by iron oxides: (a-b) Fe_3O_4, (c-d) α-Fe_2O_3,(e-f) γ-Fe_2O_3, (g-h) α-FeOOH, (j-k) γ-FeOOH.

References

1 B. Ravel and M. Newville, ATHENA, ARTEMIS, HEPHAESTUS: data analysis for X-ray absorption spectroscopy using IFEFFIT, *J Synchrotron Radiat*, 2005, **12**, 537–541.

2 H. Funke, A. C. Scheinost and M. Chukalina, Wavelet analysis of extended x-ray absorption fine structure data, *Phys. Rev. B*, 2005, **T115**, 232–234.

3 P. Haas, F. Tran, P. Blaha, L. S. Pedroza, A. J. R. Da Silva, M. M. Odashima and K. Capelle, Systematic investigation of a family of gradient-dependent functionals for solids, *Phys. Rev. B*, 2010, **81**, 125136–125136.

4 M. Capdevila-Cortada, Z. Łodziana and N. López, Performance of DFT+U Approaches in the Study of Catalytic Materials, *ACS Catal.*, 2016, **6**, 8370–8379.

5 D. L. A. De Faria, S. Venâncio Silva and M. T. De Oliveira, Raman microspectroscopy of

some iron oxides and oxyhydroxides, *J. Raman Spectrosc.*, 1997, **28**, 873–878.

6 Y.-S. Li, J. S. Church and A. L. Woodhead, Infrared and Raman spectroscopic studies on iron oxide magnetic nano-particles and their surface modifications, *J. Magn. Magn. Mater.*, 2012, **324**, 1543–1550.